Results in Engineering 24 (2024) 103432

Contents lists available at ScienceDirect

Results in Engineering

journal homepage: www.sciencedirect.com/journal/results-in-engineering

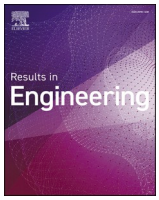

Utilizing supercritical water gasification for hydrogen production combined with a waste heat recovery system for domestic households

Sathish Thanikodi [a,*], Atul A. Sagade [b]

[a] Department of Mechanical Engineering, Saveetha School of Engineering, SIMATS, Chennai, Tamil Nadu, India
[b] Departamento de mecánica, Universidad de Tarapaća, Arica, Chile

ARTICLE INFO

Keywords:
Sustainable energy, waste, Building heating
Food waste and Proton exchange membrane

ABSTRACT

Hydrogen from food waste can provide sustainable energy. Food waste can be gasified into clean, efficient hydrogen gas using cutting-edge techniques. This study is about the gasification of food waste under different settings to determine gas production and efficiency. The supercritical water gasification (SCWG) method was used in experiments at 400 °C, 450 °C, and 500 °C with reaction durations of 30, 60 and 90 min. The results showed peak values of CO_2, CO, CH_4, H_2 at 90 min, equivalent to 6.2 % and 7.9 % hydrogen efficiency (HE) and cold gas efficiency (CGE). Peak CGE and HE were 6.7 % and 9.2 % at 500 °C, whereas peak CE and total gas output were 6.8 % and 8.6 %. To generate heat and power, a PEM cell was added. Gasification-generated hydrogen was warmed and fed in the PEM circuit at 0.7, 1 and 1.5 m/s. The peak velocity indicates a 23.1 % waste heat recovery rate and a higher hydrogen temperature difference of roughly 8.1 °C. At the temperature of peak gasification (500 °C), the values of CO_2, CO, CH_4, and H_2 are approximately 3.6 mol/kg, 0.3 mol/kg, 2.6 mol/kg, and 4.7 mol/kg, respectively. At the peak gasification temperature (500 °C), As a result, the suggested system is ideal for combining hydrogen production to generate both power and heat energy for use in heating small homes or buildings (the proposed system can deliver that much energy or at least partially fulfill it).

1. Introduction

Large-scale waste production and the depletion of energy resources are two significant issues brought on by population growth [1,2]. Hydrogen is regarded as a cleaner and renewable energy source that can be used to compensate energy needs [3,4]. Therefore, producing hydrogen from renewable sources and increasing its global generation is very interesting [5]. The development of a series of energy conversion techniques, including biomass thermochemical conversion technologies like torrefaction, pyrolysis, hydrothermal liquefaction, or gasification, was prompted by the search for alternatives to conventional fossil energy sources [1]. In order to produce hydrogen-rich syngas, thermodynamic modelling was used to simulate the co-gasification of biomass and plastic waste. Up to a five plastic-to-biomass ratio improves CO and hydrogen yields and raises the gas's HHV from 21 to 25 MJ/kg [2]. In order to maximise the production of syngas from the catalytic steam gasification of bamboo biomass in a two-stage fixed-bed reactor, the reusability potential of Ni/char catalyst was investigated using one unmodified (Ni/MMchar) and two modified catalysts (Ni/NaMMchar and Ni/NaAceMMchar) [3]. Even though the bed material was changed for each experiment, beechwood was always utilised as the biofuel. In the study, four different kinds of bed materials—silica sand, olivine, Na–Y zeolite, and ZSM-5 zeolite—were used, and a steady steam injection was kept up. In steady-state conditions, the ZSM-5 Zeolite produced the greatest amounts of hydrogen [4]. In a bench-scale rotary kiln, grains of hazelnut shell are gasified at 800 °C using air as the gasifying agent. In order to lessen the load of contaminants, the producer gas is directly treated in a thermal cleaning unit that runs between 800 and 1100 °C. The development of a series of energy conversion techniques, including biomass thermochemical conversion technologies like torrefaction, pyrolysis, hydrothermal liquefaction, or gasification, was prompted by the search for alternatives to conventional fossil energy sources [5].

Integrating energy sources for sustainable development is widely discussed in the literatures. In order to solve the sizing problem for an on-grid hybrid renewable energy system (HRES) consisting of solar photovoltaic (PV) panels, diesel generators (DG), wind turbines (WT), and battery storage systems (BSS), [6] introduced an optimisation model and assessed the effectiveness of various metaheuristic optimisation techniques. A university campus was chosen as the case study location in

* Corresponding author.
E-mail addresses: sathisht.sse@saveetha.com (S. Thanikodi), atulsagade@gmail.com (A.A. Sagade).

https://doi.org/10.1016/j.rineng.2024.103432
Received 19 September 2024; Received in revised form 3 November 2024; Accepted 14 November 2024
Available online 15 November 2024

order to evaluate the suggested HRES's efficacy. [7] generated electricity from a hybrid energy production system with solar panels, wind turbine, diesel generator, and battery components, reducing the carbon emissions of a university campus. The load demands, wind speed, solar radiation, and ambient temperature on the university campus where the hybrid energy system was installed have all been entered into our database. Using this data, optimisation algorithms were utilised to choose, in an economical and efficient manner, the power values of the system components that should be installed, taking into account the surrounding environment. Using MATLAB/Simulink, the grey wolf optimiser combined with cuckoo search (GWOCS) technique was investigated for the best way to size the HRES components.

[8] provided a complex framework that highlighted energy modules like fuel cells, solar power, biomass gasification, wind, and solar energy systems optimization and energy flow management. Hydrogen, which could be stored, was created from excess energy and used in fuel cells. One crucial factor in their optimization process is the Annual Cost of the System (ACS). [9] looked into the techno-economics of off-grid fuel cell (FC), biomass gasifier (BG), solar (PV), and wind (WT) systems. These systems store excess solar and wind energy and use it to create hydrogen, which powers fuel cells. From a practicality perspective, it is crucial. In order to optimize and compare hybrid and off-grid charging stations for electric vehicles across six different regions, [10] estimated that the station will produce 3049,337 kWh of energy annually. For the best component sizing, the Harmony Search (HS) algorithm was employed by Güven et al. [11] and contrasted with alternative approaches. Photovoltaic (PV), wind turbine, battery, diesel generator, and inverter components made up the Hybrid Renewable Energy Systems. [12] concentrated on integrating an advanced hybrid metaheuristic technique into a hybrid renewable energy system created especially for a Turkish university campus. A variety of technologies, such as photovoltaic (PV) panels, wind turbines, batteries, diesel generators, and inverters, are combined in the developed HRES. Our work includes a novel approach: we implement an Energy Management Scheme with rules to efficiently coordinate the power flow among various system components. Using HOMERPro software, [13] designed a hybrid energy system with solar, wind, diesel generators, and battery components to meet the electricity needs of the closed prison in Balikesir's Burhaniye district. Five distinct battery scenarios were applied to the hybrid energy system during simulations, and the best outcome was found. Using HOMER-Grid software, optimised electric vehicle charging stations (EVCS) powered by renewable energy sources are identified as the most efficient scenario out of seven resource-based scenarios [14]. Specifically, Scenario 3, which brought together the grid-connected solar power systems. The technical and financial aspects of a hybrid microgrid located at a specific latitude of 40°39.2′N and longitude of 29°13.2′E, that is integrated with different components like photovoltaic panels (PVs), wind turbines (WTs), battery energy storage systems (BESSs), and electric vehicle grid connections. The used methodology is based on sophisticated stochastic metaheuristic techniques. Two different loads are supported by the infrastructure: one for primary use and another for EV charging [15]. [16] examined the optimisation of a hybrid energy system that was connected to the grid and included battery and supercapacitor storage in addition to photovoltaic (PV) and wind turbine (WT) components. The study tackles the vital requirement for effective energy storage methods in the integration of renewable energy sources.

The production of hydrogen from waste has great potential to address the issues of waste management and the demand for renewable energy sources [17–19]. Hydrogen gas a flexible and environmentally friendly fuel can be produced by harnessing the energy potential found in various waste materials [20]. Modern methods such as gasification, pyrolysis, and biochemical conversion can efficiently transform a variety of organic waste streams, such as wastewater sludge, municipal solid waste, and agricultural residues, into hydrogen-rich syngas [21]. In particular, the conversion of food waste into hydrogen via water gasification proved to be a wise decision, yielding syngas with a high hydrogen content. This procedure helps achieve the goals of renewable energy and sustainable waste management by keeping food waste out of landfills and producing valuable clean energy [22].

The physicochemical characteristics of a variety of common food wastes and how well they performed during steam gasification were greatly impacted by torrefaction [23]. According to the study, torrefaction significantly improved the fuel quality of conventional food waste, and the best temperature for torrefaction to maximize waste upgrading was found to be 280 °C [24]. The overall exergy efficiency of the integrated process was shown to be similar to the direct gasification of wood was investigated by Prins et al. [25]. They also noticed that the combined process's resulting gas's chemical exergy was 5.8 % greater than direct gasification's. A hydrogen generation system using pre-dried food waste gasification (10 t/h) [26]. it demonstrated a noteworthy exergy efficiency of 64.86 %.

Supercritical water gasification, unlike conventional thermochemical gasification, obviates the necessity for drying and proves to be an efficient means of converting wet biomass into hydrogen [27] [28]. Water attains a supercritical state when its temperature exceeds 374 °C and pressure surpasses 22.1 MPa [29]. Exhibiting dielectric constant, polarity, low viscosity, and supercritical water demonstrates remarkable diffusivity, reactivity and solubility [30]. Fructose was gasified at 700 °C and 25 MPa for waste fruit and vegetable [31]. Without the aid of a catalyst, they were able to produce the maximum hydrogen production of 3.37 mol/mol. The duration of the reaction, temperature, and raw material concentration are some of the variables that affect how efficient the gasification process is. The quantity and quality of the synthesis gas produced are influenced by these factors combined [32]. The SCWG temperature increases can produce large amounts of hydrogen (H_2), with the concentration of H_2 rising from 5.40 % to 38.95 % [33]. Furthermore, the SCWG process's residence time for feedstock has a big influence on how much hydrogen is produced. A longer residence period is necessary in the gasification process to enable sufficient progression of the first hydrolysis reaction due to the complex composition of food waste [34].

Furthermore, the process of hydrogen for the heating application could probably be used through the cell. Hence, the Proton Exchange Membrane (PEM) fuel cell acts as a generator for power production and heat during the process of the cell using hydrogen [35]. Under typical operating conditions, the PEM fuel cell stack's energy conversion efficiency is between 40 % and 50 % [36]. The primary causes of heat generation are ohmic resistance, exothermic water creation, entropy transition from reactants to products and reaction irreversibility [37].

While lower-quality waste heat from PEM fuel cells at low temperatures may limit their direct applications, they remain suitable for generating low-pressure steam or hot water [38]. Automotive applications demonstrate the use of high-performance nanostructured Thermoelectric Generators (TEGs) operating above 300 °C, even when waste heat temperatures are approximately 60 °C [39]. Additionally, recent developments include the utilization of a vacuum thermionic generator for heat recovery at temperatures ranging from 600 to 800 °C [40]. Scaling and customizing these advanced technologies, alongside improved traditional waste energy harvesting methods like solar chimneys [41], could optimize energy recovery in low-temperature systems. Exploring creative applications of Combined Heat and Power (CHP), such as powering commercial greenhouses [42], could further advance the concept.

From the above literature, utilizing waste materials for hydrogen production shows significant promise and feasibility. Several research endeavours have investigated diverse methodologies including gasification, supercritical water gasification, and thermochemical processes for converting waste into hydrogen gas. The essential factors such as reaction duration, gasification temperature, and waste material composition profoundly influence the efficiency and output of hydrogen production. Moreover, advancements in technologies like PEM fuel cells, are being pursued to optimize energy recovery from waste heat.

But both the combined systems were not available. Furthermore, the energy consumption for heating small houses must be considered to achieve this building heating. In this investigation, the hydrogen production of the super-critical water gasification was studied under various operating conditions. The gasification was conducted at a reaction time of about 30 min, 60 min, and 90 min, and the gasification temperature of about 400 °C, 450 °C, and 500 °C. Also, the PEM cell is integrated for power and heat supply through the produced hydrogen from the gasification process. For building heating, the integrated system utilizes the heat energy generated from the gasification process, facilitated by the PEM cell. The produced hydrogen is employed as a fuel source to generate both electricity and heat. In conclusion, the higher reaction time, and gasification temperature show the peak H_2 generation. Furthermore, the hydrogen with 1.5 m/s flow velocity in the PEM cell circuit shows maximal heat energy to the system. Hence, this proposed system can deliver the required heat and power energy, or at least partially meet the heating needs of the building.

2. Material and methods

SWGR batch reactors with 300 ml capacities were used for gasification. The essentials of the reactor controller, water supply, electrical furnace, biomass feeder, transducer, pressure gauge, control valve, and gas cylinder were equipped. The reactor was made of 300 ml capacity stainless steel and integrated into a data logging system to control and monitor temperature and pressure during gasification. The specific reaction times and temperatures (30, 60, 90 min and 400 °C, 450 °C, 500 °C) were chosen based on the trial and error type pertest for optimizing these parameters to maximize the H_2 production,

Fig. 1 illustrates the overall supercritical water gasification process H_2 production. The details are as follows.

Biomass and Water Storage: Biomass is fed into the gasifier through a controlled biomass feeder system. Water is supplied from a storage tank, and both these inputs are essential for the gasification process.

SWGR Batch Reactors: The reactor used in this experiment is made of stainless steel, with a capacity of 300 ml. It is a controlled system where temperature and pressure are monitored using a transducer, pressure gauge, and data logging system. The reactor can operate under a maximum working pressure of 20 Mpa and a maximum temperature of 650 °C.

Electrical Furnace: An electrical furnace is utilized to heat the reactor during gasification. The temperatures used in the experiment are 400 °C, 450 °C, and 500 °C, tested over specific durations of 30, 60, and 90 min. The furnace ensures the reaction temperature is consistent.

Hydrogen Gas Storage and Supply: The hydrogen produced during the gasification process is stored in a cylinder. The stored hydrogen is then preheated before being supplied to a fuel cell system.

Fuel Cell System: The hydrogen gas is fed into an Open-Cathode Polymer Electrode Membrane (PEM) fuel cell stack. This fuel cell stack operates with air as both the reactant and coolant. The stack outflow air is hotter than the ambient temperature, which influences the fuel cell's performance. The heat generated can be used for heating applications (building heat supply), and the electrical output can be used to power small homes. The cooling of the stack is controlled by adjusting the air velocity. The air velocities tested are 0.7, 1.0, and 1.5 m/s. The effect of these velocities on the stack's temperature was monitored, and heat exchange between the stack air and hydrogen was influenced by these variations.

Electronic Loader: The fuel cell system was attached to a 60 A electrical load, which helped in generating the stack polarization profile. This load mimics real-world electricity consumption, allowing for the study of the fuel cell's performance under different operational conditions.

2.1. Food waste preparation

The daily food waste samples were collected from our institution's hostel. Thus, waste includes grains, oil, vegetables, etc. [43]. Therefore, the reactants are 10 wt% protein powder, 20 wt% cooking oil, 30 wt% cellulose, and 40 wt% soluble starch. Protein powder, Sodium hydroxide, sodium bicarbonate, and sodium chloride were procured from Sinopharm Chemical Reagent Co., Ltd. The cellulose and soluble starch were procured from Bio Reliance, solution Technology India. Co., Ltd. The ultimate and proximate food waste analyses are provided in Table 1.

Table 1
Analysis of food samples used for this investigation.

Parameter	Unit	Value
H2 (Hydrogen)	%	9.6
C (Carbon)	%	34.25
S (Sulfur)	%	0.2
N (Nitrogen)	%	2.7
Total solid	%	59.34
pH	No	4.6

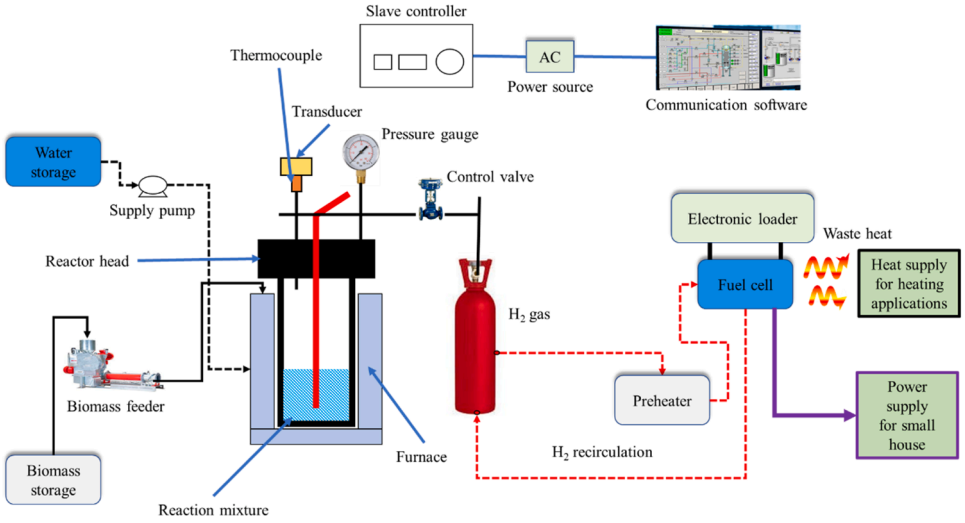

Fig. 1. Schematic diagram of overall supercritical water gasification process H_2 production.

2.2. Experimental procedure

The gasification experiments were done in a stainless-steel batch reactor and the quartz glass container was integrated into the reaction tank. The model chemical was combined with distilled water to 50 ml following the experiment's proportions and charged into the reactor. Magnetic stirring at 200 rpm was used to agitate the reaction mixture. To create an oxygen-free atmosphere inside the reactor, high-purity argon was purged for 2 min before the reaction began. The reactor was heated to a specified temperature (400–500 °C) at a rate of 10 °C/min using an electric heating furnace. The reactor pressure ranged from 25 to 30 MPa after attaining the target temperature. Different residence periods (30–120 min) were used for the reaction, depending on experimental circumstances. After the experiment, the reactor was cooled to room temperature using a water-cooling ring. The produced gas was collected using an airbag, quantified for volume, and analyzed using gas chromatography for composition. Similarly, Fig. 2 shows the graphical representation of the current study.

A centrifuge tube was used to collect the residual liquid and solid residue in the reaction vessel for further investigation. All experiments ran simultaneously for each reaction duration and different temperature conditions. Hydrogen was supplied by the fuel cell. A preheater heated hydrogen before the fuel cell. PEM fuel cells should have a hydrogen stoichiometry of 2 at 15 A to avoid hydrogen starvation. Here, 15 A is the maximum load current. The steady-state stack temperature controls the load change period, which is usually <5 min for 0–5 A load and increases as the current load increases (about 10 min at 15 A). The load was increased after recording the relevant data at the steady-state stack temperature. Table 2 shows the specifications of the system.

Furthermore, cold gas efficiency (CGE) is defined as the ratio of energy available in the total syngas to the feedstock feedstock's total energy. Hence, the CGE, Total gas yield, gas yield, gas fraction, H_2 selectivity, hydrogen efficiency (HE), and carbon efficiency (CE) were calculated by using the following equations from (1) to (6) [44].

$$CGE(\%) = \frac{m(food\ waste)LHV\ gas}{\sum m\ (i)LHV\ (i)} \tag{1}$$

$$Total\ gas\ yield = gas\ yield\ CH_4 + gas\ yield\ H_2 + \ gas\ yield\ CO_2 + gas\ yield\ CO \tag{2}$$

$$Gas\ yield\ \left(\frac{mol}{kg}\right) = \frac{Gaseous\ product\ moles}{Total\ mass\ of\ food\ waste} \tag{3}$$

$$H_2\ selectivity\ (\%) = \frac{H_2\ mole}{sum\ of\ CH_4,\ H_2,\ CO, CO_2} \times 100\% \tag{4}$$

$$HE(\%) = \frac{Hydrogen\ total\ mass\ in\ gaseous\ product}{Hydrogen\ total\ mass\ in\ food\ waste} \times 100\% \tag{5}$$

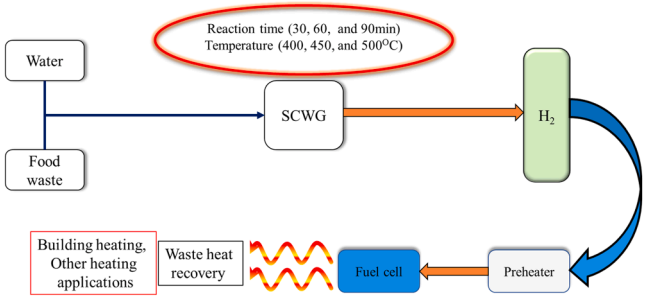

Fig. 2. Graphical representation of the current study of overall supercritical water gasification process H_2 production from food waste.

Table 2
Specification of the system.

Parameter	Value
Hydrogen pressure P_{H2}	0.3 bar
Oxygen pressure P_{O2}	0.21 bar
Area of the system A	100 cm^2
Maximum current I_{Max}	33A
Stack temperature T_{st}	320K
Hydrogen stoichiometry, S_{H2}	2

$$CE(\%) = \frac{Carbon\ total\ mass\ in\ gaseous\ product}{Carbon\ total\ mass\ in\ food\ waste} \times 100\% \tag{6}$$

Hence, the $m\ (i)$ is the mass of food waste. Table 3 provides a list of the primary test equipment and their accuracy. The process is based on Holman's uncertainty analysis [45], which states that the accuracy of each measured condition within a parameter contributes to its uncertainty. Based on the uncertainty in the measurements of all relevant independent variables, the uncertainty analysis was computed.

2.3. Uncertainty analysis

In the measurement findings of the gasification process, the uncertainty value of the measured quantities was estimated by using Eq. (7).

$$u = a/\sqrt{3} \tag{7}$$

$$U(\eta) = \eta\left[\left(\frac{u(m)}{m}\right)^2 + \left(\frac{u(I_b)}{I_b}\right)^2\right]^{\frac{1}{2}} \tag{8}$$

Where, u and a are the precision of the measurement device and the standard uncertainty value. Based on Eq. (8), the combined uncertainty for hourly-based value was estimated. The IBM SPSS software v 26 was employed in this investigation for data analysis.

3. Result and discussion

This study examined the water gasification of food waste under various operating conditions. The reaction durations ranged from approximately 30 to 90 min, and the temperatures were between 400 °C and 500 °C. The analysis focused on gasification efficiency, gas yield, and hydrogen production efficiency. Additionally, the hydrogen produced was used for heat generation through a PEM (Proton Exchange Membrane) cell at different hydrogen flow velocities.

3.1. Reaction time

In this study, the reaction time for the gasification of food waste was a key variable, ranging from 30 to 90 min. For, the reaction time variation, the gasification temperature was set to gasifier temperature (400 °C) as shown in Fig. 3**(a)**. The different gas yields for different reaction temperatures with error bars at 95 %, were comparatively presented in Fig. 3(a). H_2 selectivity values were also plotted for each reaction temperature. This duration was crucial in evaluating the efficiency of

Table 3
Parameters and accuracy of test instruments.

Instruments	Model	Accuracy
DC transducer	LA 55-P/SP1	±1.9 %
Anemometer	AVM-03	±2 %
Thermocouple	K-thermocouple RS PRO	±0.5 %
Digital hydrogen flow meter	AMS2106	±0.7 %
Pressure gauge	WIKA 232.50/233.50 Bourdon Tube Pressure Gauge	±0.5 %

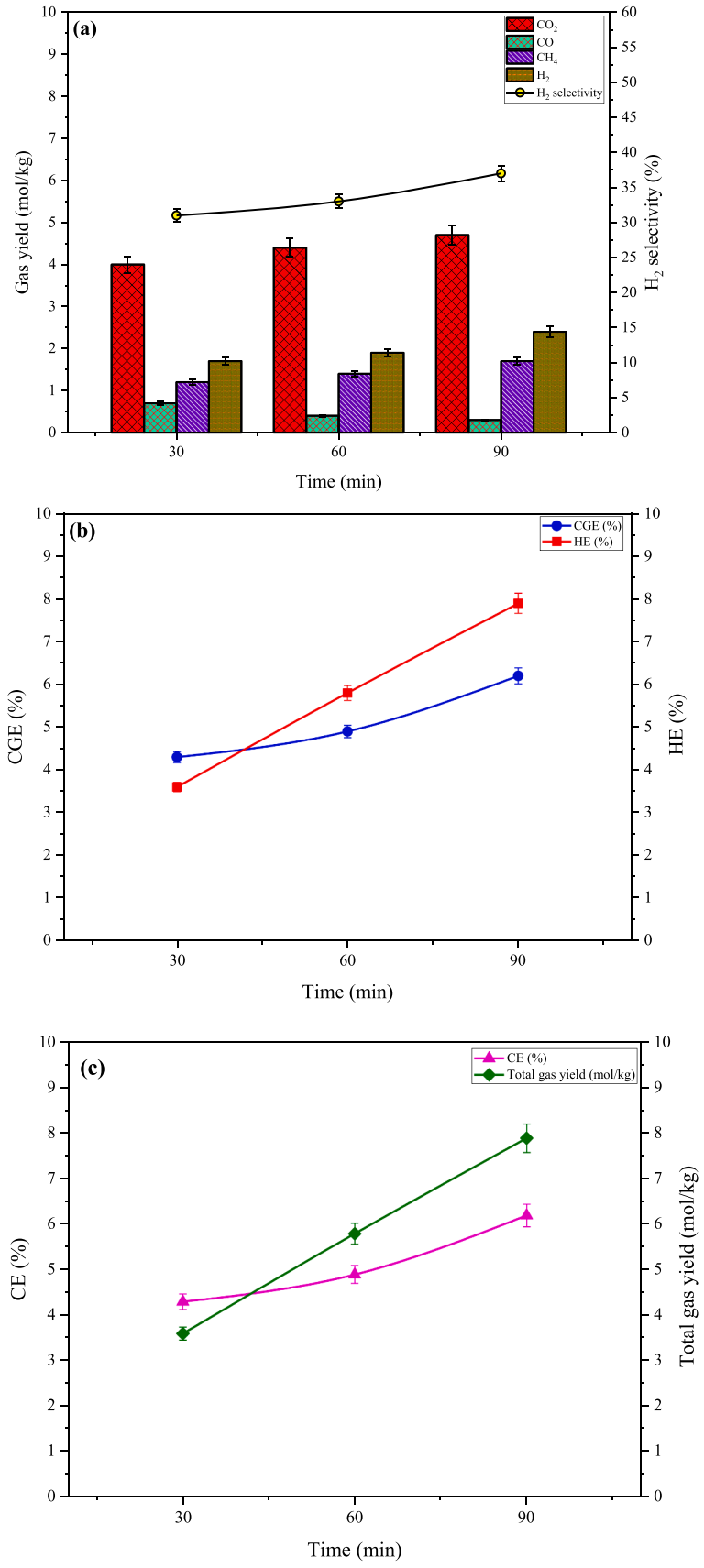

Fig. 3. Effect of reaction time on: (a) Different gas yields with error bars at 95 % CI and selectivity; (b) CGE, and HE; (c) CE, and Total gas yield.

gasification, the yield of gas produced, and the efficiency of hydrogen production. Because of the food waste in the gasifier based on the reaction time for the gasification process. During the gasification, the CO was decreased, and the other gases CO_2, H_2, and CH_4 were increased as the reaction time increased. The peak values of CO_2, CO, CH_4, and H_2 are about 4.7 mol/kg, 0.3 mol/kg, 1.7 mol/kg, and 2.4 mol/kg was recorded at higher reaction times (90 min). Similarly, the H_2 selectivity is about 37.1 % at the same reaction duration. The error bars were drawn at ± 1SD. The standard deviation of the sample data for each category is represented by a bar. The error bar will extend one standard deviation above and below the mean value to show the variability or spread of data in a sample. The Standard Error of the Mean (SEM) was estimated to show how accurately the sample mean represents the population mean. To calculate this, the standard deviation is then divided by the square root of the sample size (n). As each observation was taken 5 times at the same settings and their average was considered for analysis, the sample size is 5. Error bars were extended by one standard error above and below the mean. This was done with IBM SPSS software.

The variation in mol/kg values during the gasification process of different food samples is influenced by their composition, including carbohydrates, fats, proteins, and moisture content [46]. High carbohydrate content increases CO production, which subsequently decreases through the water-gas shift reaction, forming CO_2 and H_2. Fats contribute more to CH_4 production via the methanation reaction due to their higher hydrogen content, reducing CO levels and increasing CH_4. Proteins, containing nitrogen, can lead to ammonia formation, indirectly affecting gas composition. High moisture content enhances the water-gas shift reaction, further lowering CO and raising CO_2 and H_2 levels. Thus, the food sample determines the extent of these reactions and the resulting gas composition. Hence, the higher reaction duration enables better combustion in the gasifier through the conversion of the feedstock, which raises total gas output [47].

Similarly, Fig. 3**(b)** depicts the variation of CGE, and HE by different reaction duration conditions. Both the CGE, and HE values were increased as the reaction duration increased [48]. The maximum CGE and HE values of approximately 6.2 % and 7.9 %, respectively, were recorded at the highest reaction times of 90 min. Because of this, longer reaction durations enable a more complete conversion of the feedstock (food waste), which raises the amount of gasses that catch fire due to effective combustion. Higher yields of gases, including CO, CO_2, H_2, and CH_4, result from extended reaction times, which allow more complete decomposition of the food sample's organic matter and enhance the water-gas shift and methanation reactions which improve CGE and HE. Longer reaction times also maximize the production of gas by giving gasification reactions enough time to achieve equilibrium [49].

In addition, the ideal parameters for hydrogen production, temperature, and pressure are maintained for an extended length of time, which improves CHE and HE values [50]. Furthermore, Fig. 3(c) shows the variation of CE, and total gas yield varied with the reaction time. It also follows the same trend (as the value increases with reaction time increases). The CE and total gas yields are about 6.2 %, and 7.9 % respectively and it was a maximum value compared to others [51,52]. The improved performance of the gasification process is indicated by the rise in both the total gas production and the CE with longer reaction durations. Extended reaction durations provide a more comprehensive conversion of the feedstock, leading to elevated yields of combustible gases and increased energy production. This is because longer times allow for the complete breakdown of organic matter, maximizing the production of CO, CO_2, H_2, and CH_4. Prolonged reactions also enhance the water-gas shift and methanation reactions, converting more CO into CO_2, H_2, and CH_4 production [45].

3.2. Gasification temperature

During the gasification process, the higher reaction time shows better conversion efficiency and total gas value than the lower reaction time. Hence, the peak reaction time (90 min) was set to be constant and the gasification temperature varied between 400 °C, 450 °C, and 500 °C. Fig. 4**(a)** depicts the variation of gas yield and H_2 selectivity with different gasification temperatures. The H_2 and CO were increased as the gasification temperature increased. CO_2 and CH_4 were decreased and then increased. The values of CO_2, CO, CH_4, and H_2 are about 3.6 mol/kg, 0.3 mol/kg, 2.6 mol/kg, and 4.7 mol/kg respectively at peak gasification (500 °C) temperature [50].

Because of improved reaction rates and thermodynamic favorability at higher temperatures, H_2, and CO concentrations rise as gasification temperatures rise. This promotes the breakdown of organic materials, which increases the amount of CO_2 and H_2 produced. The concentrations of CO_2 and CH_4 decreased and then increased, which can be explained by the several gasification reactions' shifting equilibrium. At first, more CO_2 and CH_4 may be used up in secondary processes as the temperature rises. Higher temperatures, however, might encourage the formation of CO_2 and CH_4 through primary gasification processes [41].

Similarly, Fig. 4**(b)** depicts the variation of CGE, and HE by different gasification temperature conditions. Both the CGE and HE values were increased as the gasification temperature increased. The peak CGE, and HE are about 6.7 %, and 9.2 % are recorded at peak gasification (500 °C) temperature. Due to higher gasification temperatures quicken the gasification operations, which makes food waste into gaseous products more effectively. Higher yields of flammable gases, such as hydrogen, are produced, improving CGE and HE. Furthermore, the kinetics of secondary reactions favor the formation of hydrogen over other byproducts at higher temperatures. Moreover, higher temperatures encourage a stronger equilibrium shift favoring desired gas products like hydrogen.

Furthermore, Fig. 4**(c)** shows the variation of CE, and total gas yield varied with the gasification temperature. It also follows the same trend (as the value increases with gasification temperature increases). The peak CE and total gas yield are about 6.8 %, and 8.6 % respectively. Hence, several parameters can contribute to the increase in CE and total gas output that occurs at higher temperatures during gasification. First off, higher temperatures quicken the gasification operations, which makes feedstock into gaseous products more effective. Higher combustible gas yields are the outcome, which enhances CE and total gas yield. Higher temperatures also encourage a stronger equilibrium shift in favor of the desired gas products, which improves gas output overall. Moreover, secondary reactions promote the formation of desirable gases, such as hydrogen, at higher temperatures [45].

3.3. Heat recovery system

From the process of hydrogen production, the produced hydrogen was further used in PEM cells for the heat production process. Hence, the hydrogen was supplied to the PEM cell under different velocities such as 0.7 m/s, 1 m/s, and 1.5 m/s. The heat produced by the air leaving the stack is used in the heat exchanger to supply the required heating power for the hydrogen preheating procedure. The hydrogen heating degree, or ΔT_{H2}, for both preheating loops at different air velocities, is shown in Fig. 5 across the heat exchanger. After attaining a particular stack load—roughly 6 A in all cases—there is a discernible rise in temperature fluctuations.

This is also when the cooling efficacy, or stack heat removal, is getting close to its maximum value. The peak hydrogen temperature difference is about 5.7 ^{O}C, 6.8 ^{O}C, and 8.1 °C respectively at 0.7 m/s, 1 m/s, and 1.5 m/s hydrogen velocity. Because the stack load reaches about 6 A, there is a noticeable increase in temperature variations. This is because the system is producing more heat, which causes the temperature differentials across the heat exchanger to become more substantial. Temperature variations increase when the cooling efficacy loses some of its ability to dissipate surplus heat as the stack heat removal approaches its maximum level [44].

The differences in cooling efficacy and heat exchange at various airflow rates are reflected in the peak hydrogen temperature variances

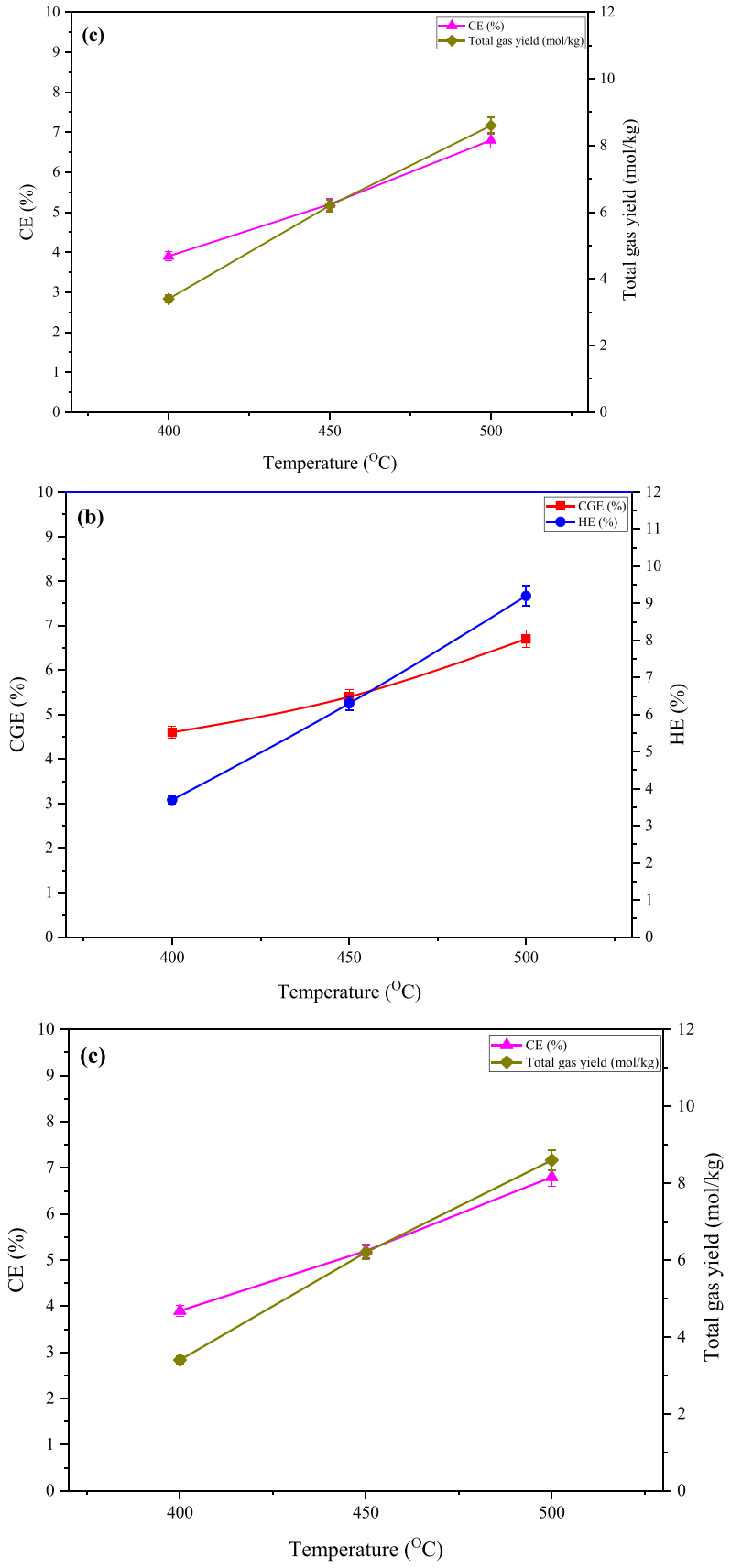

Fig. 4. Effect of gasification temperature on: (a) Gas yield, and selectivity; (b) CGE, and HE; (c) CE, and Total gas yield.

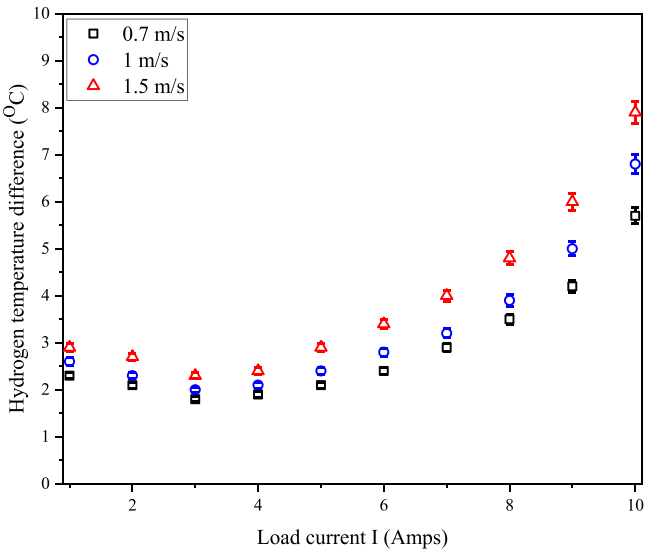

Fig. 5. The influence of air velocity to the hydrogen preheating degree at the heat exchanger.

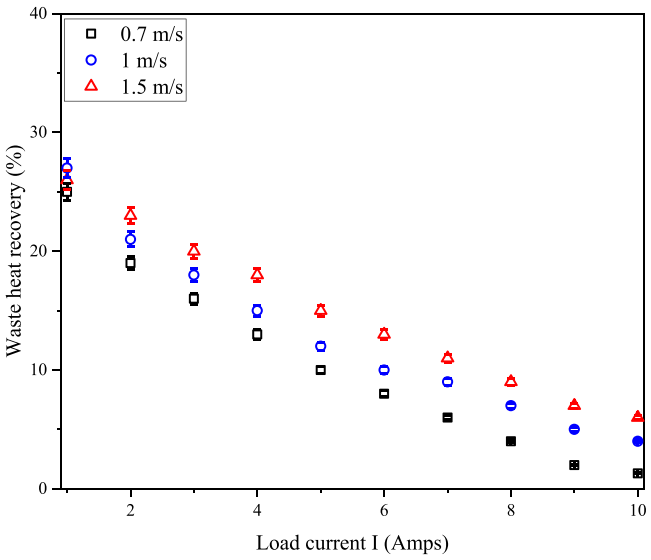

Fig. 7. Waste heat recovery by the system from the PEM cell.

at various hydrogen velocities. Similarly, Fig. 6 shows the heat rate by the different hydrogen supply flow rates in the heat from the PEM cell. The peak heat rate by 0.7 m/s, 1 m/s, and 1.5 m/s hydrogen velocity is about 79.2 °C, 81.9 °C, and 89.3 °C respectively. Higher hydrogen velocities cause an increase in peak heat rate, which is explained by increased heat transfer rates inside the system. More hydrogen flows through the heat exchanger as hydrogen velocity rises, enabling more effective heat exchange between the hydrogen and the air. Peak heat rate rises as a result of a faster rate of heat transfer from the air to the hydrogen. Increased heat dispersion and mixing within the system could be facilitated by higher hydrogen velocities, further boosting heat transfer efficiency. Consequently, as the data shows, the peak heat rate rises steadily as the hydrogen velocity increases. The waste heat recovery percentage from the PEM cell was examined [44] using the two profiles mentioned above as a basis.

The peak heat recovery is about 18.7 %, 21.2 %, and 23.1 % respectively at 0.7 m/s, 1 m/s, and 1.5 m/s as shown in Fig. 7. There are various reasons for the rise in the waste heat recovery percentage at higher hydrogen velocities. First off, faster hydrogen velocities increase the PEM cell's internal heat transfer rates, which makes waste heat recovery more effective.

Furthermore, as hydrogen velocities rise, the system's heat mixing and distribution improve, maximizing the use of thermal energy. This raises the PEM cell's overall heat recovery efficiency. Furthermore, higher hydrogen velocities may reduce heat losses due to shorter residence times, allowing more heat to be captured and utilized. Consequently, the waste heat recovery percentage increases progressively with increasing hydrogen velocity, as observed in the provided data. Similarly, Table 4 shows the comparison of the current study with published works. Simialrly, Table 5 shows the measured value uncertainty of the current experimentation.

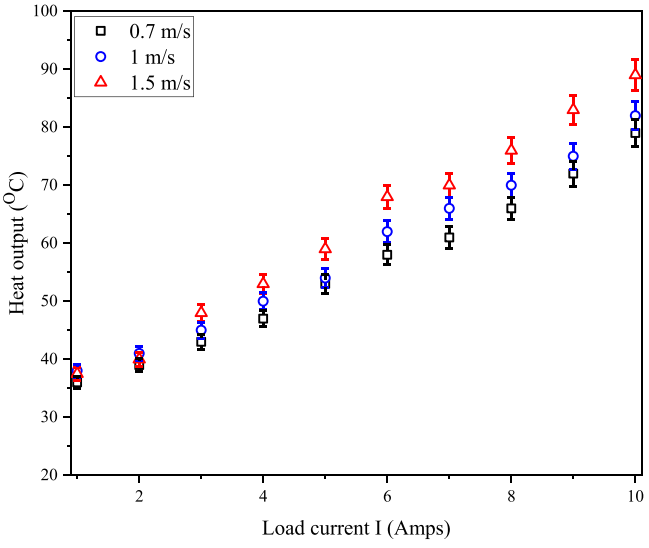

Fig. 6. Variation of heat rate by different hydrogen velocities.

4. Conclusion

The integration of supercritical water gasification (SCWG) for hydrogen production with a waste heat recovery system has promising potential for domestic energy solutions, particularly for small households. The study demonstrated that the optimal gasification conditions (500 °C and 90-minute reaction time) resulted in significant hydrogen yields and efficient heat recovery, with a peak waste heat recovery rate of 23.1 %. The result of peak hydrogen efficiency (HE) and cold gas efficiency (CGE) were determined to be 7.9 % and 6.2 %, respectively, with significant quantities of CO2, CO, CH4, and H2 at higher reaction duration. At a temperature of 500 °C, peak carbon efficiency (CE) and total gas production were 6.8 % and 8.6 %, respectively. CGE and HE peaked at 6.7 % and 9.2 %, respectively. The highest velocity (1.5 m/s)) resulted in a remarkable difference in hydrogen temperature of 8.1 °C and a waste heat recovery rate of 23.1 %.

These findings highlight the system's capacity to simultaneously

Table 4
Comparison of the studies related to waste food processing for hydrogen.

References	Additives	Process	Conversion
Sunyota et al. [53]	Biochar	Batch reactor 60 mL volume	26 %
Pagliaccia et al. [54]	Olive husks	Batch reactor 0.3 L volume	15.8 %
Zhang et al. [55]	Lime mud	Batch reactor 270 mL volume	53 %
Lin et al. [56]	Pulp & paper sludge (PPS)	Batch reactor 800 mL volume	27.6 %
The current study	Sodium hydroxide	Batch reactor 300 mL volume	23.1 %

Table 5
Measured value uncertainty.

Parameters	Measured uncertainty (%)
Gas fraction	2.6
CGE	2.5
HE	3.1
CE	3.3
H2 selectivity	2.8
Total gas yield	2.2
gas yield	3.6

generate both hydrogen for electricity and waste heat for heating purposes, making it a practical solution for energy demands in residential settings.

Implementing this integrated system on a larger scale could lead to substantial cost savings for homeowners by reducing reliance on traditional energy sources. The combined heat and power (CHP) system can potentially lower household energy bills by utilizing food waste, which is often discarded, thus converting waste into valuable energy. Additionally, the use of hydrogen as a clean fuel reduces carbon emissions, aligning with global sustainability goals.

From an economic perspective, scaling up this system could lower the costs of hydrogen production by making use of readily available food waste and improving the efficiency of heat recovery. The integration of waste heat into domestic heating systems further enhances the overall efficiency of energy use. This dual-purpose system, once refined, could offer significant environmental and financial benefits, potentially leading to widespread adoption in residential and small-scale commercial applications.

CRediT authorship contribution statement

Sathish Thanikodi: Writing – review & editing, Writing – original draft, Visualization, Validation, Supervision, Software, Resources, Project administration, Methodology, Investigation, Funding acquisition, Formal analysis, Data curation, Conceptualization. **Atul A. Sagade:** Writing – review & editing, Supervision, Resources, Methodology, Formal analysis, Data curation, Conceptualization.

Declaration of competing interest

The authors declare that they have no known competing financial interests or personal relationships that could have appeared to influence the work reported in this paper.

Limitations and future scope

The system's practical applications in building heating and efficient hydrogen production are highlighted by these results. Therefore, with less financial concern, this system may provide the necessary heat energy for construction applications. The ability of the system to gather waste heat and use it for heating increases overall efficiency and utility. Thus, by tackling energy and environmental issues simultaneously, this integrated approach offers a workable path towards renewable energy solutions.

Data availability

The data that has been used is confidential.

References

[1] L.J. Nunes, Biomass gasification as an industrial process with effective proof-of-concept: a comprehensive review on technologies, processes and future developments, Results. Eng. 14 (2022) 100408, https://doi.org/10.1016/j.rineng.2022.100408.
[2] M. Kaydouh, N. El Hassan, Thermodynamic simulation of the co-gasification of biomass and plastic waste for hydrogen-rich syngas production, Results. Eng. 16 (2022) 100771, https://doi.org/10.1016/j.rineng.2022.100771.
[3] R. Tipo, Y. Chimupala, N. Tippayawong, N. Duongbia, S. Chaiklangmuang, Feasibility of sustainable reusability of Ni/char catalyst for synthetic gas production via catalytic steam gasification, Results. Eng. 23 (2024) 102434, https://doi.org/10.1016/j.rineng.2024.102434.
[4] C. Freda, E. Catizzone, A. Villone, G. Cornacchia, Biomass gasification in rotary kiln integrated with a producer gas thermal cleaning unit: an experimental investigation, Results. Eng. 21 (2024) 101763, https://doi.org/10.1016/j.rineng.2024.101763.
[5] C. Freda, E. Catizzone, A. Villone, G. Cornacchia, Biomass gasification in rotary kiln integrated with a producer gas thermal cleaning unit: an experimental investigation, Results. Eng. 21 (2024) 101763, https://doi.org/10.1016/j.rineng.2024.101763.
[6] Aykut Fatih Güven, Heuristic Techniques and Evolutionary Algorithms in Microgrid Optimization Problems, Book Chapter, CRC Press, Microgrid, 2024, https://doi.org/10.1201/9781003481836-16 eBook ISBN9781003481836.
[7] A.F. Güven, N. Yörükeren, O.Ö. Mengi, Multi-objective optimization and sustainable design: a performance comparison of metaheuristic algorithms used for on-grid and off-grid hybrid energy systems, Neural Comput. Appl. 36 (2024) 7559–7594, https://doi.org/10.1007/s00521-024-09585-2.
[8] A.F. Güven, O.Ö. Mengi, Assessing metaheuristic algorithms in determining dimensions of hybrid energy systems for isolated rural environments: exploring renewable energy systems with hydrogen storage features, J. Clean. Prod. 428 (2023) 139339, https://doi.org/10.1016/j.jclepro.2023.139339.
[9] A. Fatih Güven, M. Mahmoud Samy, Performance analysis of autonomous green energy system based on multi and hybrid metaheuristic optimization approaches, Energy Convers. Manage 269 (2022) 116058, https://doi.org/10.1016/j.enconman.2022.116058.
[10] A.F. Güven, E. Yücel, Application of HOMER in assessing and controlling renewable energy-based hybrid EV charging stations across major Turkish cities, Int. J. Energy Stud. 8 (4) (2023) 747–780, https://doi.org/10.58559/ijes.1324236.
[11] A.F. Güven, N. Yörükeren, M.M. Samy, Design optimization of a stand-alone green energy system of university campus based on jaya-harmony search and ant colony optimization algorithms approaches, Energy 253 (2022) 124089, https://doi.org/10.1016/j.energy.2022.124089.
[12] A.F. Güven, N. Yörükeren, E. Tag-Eldin, M.M Samy, Multi-objective optimization of an islanded green energy system utilizing sophisticated hybrid metaheuristic approach, IEEe Access. 11 (2023) 103044–103068, https://doi.org/10.1109/ACCESS.2023.3296589.
[13] A.F. Güven, Ş. Türkmen, E. Aşıklı, G. Örnek, Investigating the effects of different types of battery impacts in energy storage systems on standalone hybrid renewable energy systems, Karadeniz Fen Bilimleri Dergisi 13 (3) (2023) 943–964, https://doi.org/10.31466/kfbd.1275823.
[14] A.F. Güven, E. Yücel, Sustainable energy integration and optimization in microgrids: enhancing efficiency with electric vehicle charging solutions, Electr. Eng. (2024), https://doi.org/10.1007/s00202-024-02619-x.
[15] A.F. Güven, Integrating electric vehicles into hybrid microgrids: a stochastic approach to future-ready renewable energy solutions and management, Energy 303 (2024) 131968, https://doi.org/10.1016/j.energy.2024.131968.
[16] A. Fatih Guven, A.Y. Abdelaziz, M. Mahmoud Samy, S. Barakat, Optimizing energy dynamics: a comprehensive analysis of hybrid energy storage systems integrating battery banks and supercapacitors, Energy Convers. Manage 312 (2024) 118560, https://doi.org/10.1016/j.enconman.2024.118560.
[17] M. Okasha, R. Hegazy, R.M. Kamel, Assessment of raisins byproducts for environmentally sustainable use and value addition, AgriEngineering 5 (3) (2023) 1469–1480, https://doi.org/10.3390/agriengineering5030091.
[18] Mathanraj Vijayaragavan, Balaji Subramanian, S. Sudhakar, L. Natrayan, Effect of induction on exhaust gas recirculation and hydrogen gas in compression ignition engine with simarouba oil in dual fuel mode, Int. J. Hydrogen. Energy 47 (88) (2022) 7635–37647, https://doi.org/10.1016/j.ijhydene.2021.11.201.
[19] J. Aravind Kumar, S. Sathish, T. Krithiga, T.R. Praveenkumar, S. Lokesh, D. Prabu, A. Annam Renita, P. Prakash, M. Rajasimman, A comprehensive review on bio-hydrogen production from brewery industrial wastewater and its treatment methodologies, Fuel 319 (2022) 123594, https://doi.org/10.1016/j.fuel.2022.123594.
[20] Jade Lui, Wei-Hsin Chen, Daniel C.W. Tsang, Siming You, A critical review on the principles, applications, and challenges of waste-to-hydrogen technologies, Renewable Sustainable Energy Rev. 134 (2020) 110365, https://doi.org/10.1016/j.rser.2020.110365. ISSN 1364-0321.
[21] K. Singh, N. Kumar, A. Bharti, P. Thakur, V. Kumar, Waste to energy conversion: key elements for sustainable waste management, in: A. Gupta, R. Kumar, V. Kumar (Eds.), Integrated Waste Management, Springer, Singapore, 2024, https://doi.org/10.1007/978-981-97-0823-9_5.
[22] Federica Cucchiella, Idiano D'Adamo, Massimo Gastaldi, Sustainable waste management: waste to energy plant as an alternative to landfill, Energy Convers. Manage 131 (2017) 18–31, https://doi.org/10.1016/j.enconman.2016.11.012. ISSN 0196-8904.
[23] Hesham A. FARAG, Mohamed M. EL-KHOLY, Mahmoud OKASHA*, Ahmed E. AZAB, Ahmed E. KHATER, Reham M. KAMEL, Development and evaluation of a continuous flow biochar unit using rice husk biomass, INMATEH - Agric. Eng. 72 (1) (2024).
[24] J. Huang, Y. Qiao, X. Wei, J. Zhou, Y. Yu, M. Xu, Effect of torrefaction on steam gasification of starchy food waste, Fuel 253 (2019) 1556–1564, https://doi.org/10.1016/j.fuel.2019.05.142.

[25] M.J. Prins, K.J. Ptasinski, F.J.J.G. Janssen, More efficient biomass gasification via torrefaction, Energy 31 (2006) 3458–3470, https://doi.org/10.1016/j.energy.2006.03.008.
[26] Z. Xu, H. Qi, D. Yao, J. Zhang, Z. Zhu, Y. Wang, et al., Modeling and comprehensive analysis of food waste gasification process for hydrogen production, Energy Convers. Manage 258 (2022) 115509, https://doi.org/10.1016/j.enconman.2022.115509.
[27] Sivamohan N. Reddy, Sonil Nanda, Ajay K. Dalai, Janusz A. Kozinski, Supercritical water gasification of biomass for hydrogen production, Int. J. Hydrogen. Energy 39 (13) (2014) 6912–6926, https://doi.org/10.1016/j.ijhydene.2014.02.125. ISSN 0360-3199.
[28] Steffen Heidenreich, Pier Ugo Foscolo, New concepts in biomass gasification, Prog. Energy Combust. Sci. 46 (2015) 72–95, https://doi.org/10.1016/j.pecs.2014.06.002. ISSN 0360-1285.
[29] Pooya Azadi, Ramin Farnood, Review of heterogeneous catalysts for sub- and supercritical water gasification of biomass and wastes, Int. J. Hydrogen. Energy 36 (16) (2011) 9529–9541, https://doi.org/10.1016/j.ijhydene.2011.05.081. ISSN 0360-3199.
[30] G. Brunner, Near critical and supercritical water. Part I. Hydrolytic and hydrothermal processes, J. Supercrit. Fluids. 47 (3) (2009) 373–381, https://doi.org/10.1016/j.supflu.2008.09.002. ISSN 0896-8446.
[31] Sonil Nanda, Sivamohan N. Reddy, Howard N. Hunter, Ajay K. Dalai, Janusz A. Kozinski, Supercritical water gasification of fructose as a model compound for waste fruits and vegetables, J. Supercrit. Fluids. 104 (2015) 112–121, https://doi.org/10.1016/j.supflu.2015.05.009. ISSN 0896-8446.
[32] Yuzhen Wang, Yitong Zhu, Zhuan Liu, Jian Su, Changqing Fang, Donghai Xu, Wenhan Song, Shuzhong Wang, Influences of operating parameters on liquefaction performances of Tetra Pak in sub-/supercritical water, J. Environ. Manage. 237 (2019) 545–551, https://doi.org/10.1016/j.jenvman.2019.02.114. ISSN 0301-4797.
[33] Dwi Hantoko, Hongcai Su, Mi Yan, Ekkachai Kanchanatip, Herri Susanto, Guobin Wang, Sicheng Zhang, Zhang Xu, Thermodynamic study on the integrated supercritical water gasification with reforming process for hydrogen production: effects of operating parameters, Int. J. Hydrogen. Energy 43 (37) (2018) 17620–17632, https://doi.org/10.1016/j.ijhydene.2018.07.198. ISSN 0360-3199.
[34] Onwudili, J.A., Williams, P.T. (2014). Production of Hydrogen from Biomass via Supercritical Water Gasification. In: Fang, Z., Xu, C. (eds) Near-critical and Supercritical Water and Their Applications For Biorefineries. Biofuels and Biorefineries, vol 2. Springer, Dordrecht. https://doi.org/10.1007/978-94-017-8923-3_11.
[35] Tabbi Wilberforce, A.G. Olabi, Imran Muhammad, Abed Alaswad, Enas Taha Sayed, Ahmed G. Abo-Khalil, Hussein M. Maghrabie, Khaled Elsaid, Mohammad Ali Abdelkareem, Recovery of waste heat from proton exchange membrane fuel cells – a review, Int. J. Hydrogen. Energy 52 (Part C) (2024) 933–972, https://doi.org/10.1016/j.ijhydene.2022.08.069. ISSN 0360-3199.
[36] X. Li, Principles of Fuel Cells, 1st ed., CRC Press, 2005 https://doi.org/10.1201/9780203942338.
[37] Amir Amirfazli, Saeed Asghari, Morteza Koosha, Mathematical modeling and simulation of thermal management in polymer electrolyte membrane fuel cell stacks, J. Power. Sources. 268 (2014) 533–545, https://doi.org/10.1016/j.jpowsour.2014.06.073. ISSN 0378-7753.
[38] Harikishan R. Ellamla, Iain Staffell, Piotr Bujlo, Bruno G. Pollet, Sivakumar Pasupathi, Current status of fuel cell based combined heat and power systems for residential sector, J. Power. Sources. 293 (2015) 312–328, https://doi.org/10.1016/j.jpowsour.2015.05.050. ISSN 0378-7753.
[39] Yanliang Zhang, Martin Cleary, Xiaowei Wang, Nicholas Kempf, Luke Schoensee, Jian Yang, Giri Joshi, Lakshmikanth Meda, High-temperature and high-power-density nanostructured thermoelectric generator for automotive waste heat recovery, Energy Convers. Manage 105 (2015) 946–950, https://doi.org/10.1016/j.enconman.2015.08.051. ISSN 0196-8904.
[40] Chuankun Huang, Yuzhuo Pan, Yuan Wang, Guozhen Su, Jincan Chen, An efficient hybrid system using a thermionic generator to harvest waste heat from a reforming molten carbonate fuel cell, Energy Convers. Manage 121 (2016) 186–193, https://doi.org/10.1016/j.enconman.2016.05.028. ISSN 0196-8904.
[41] Kai Chen, Jiangfeng Wang, Yiping Dai, Yuqi Liu, Thermodynamic analysis of a low-temperature waste heat recovery system based on the concept of solar chimney, Energy Convers. Manage 80 (2014) 78–86, https://doi.org/10.1016/j.enconman.2014.01.007. ISSN 0196-8904.
[42] Amir Vadiee, Mahmoud Yaghoubi, Marco Sardella, Pardis Farjam, Energy analysis of fuel cell system for commercial greenhouse application – a feasibility study, Energy Convers. Manage 89 (2015) 925–932, https://doi.org/10.1016/j.enconman.2014.09.073. ISSN 0196-8904.
[43] Francesca Girotto, Luca Alibardi, Raffaello Cossu, Food waste generation and industrial uses: a review, Waste Manag. 45 (2015) 32–41, https://doi.org/10.1016/j.wasman.2015.06.008. ISSN 0956-053X.
[44] W.A.N.W. Mohamed, M. Haziq M. Kamil, Hydrogen preheating through waste heat recovery of an open-cathode PEM fuel cell leading to power output improvement, Energy Convers. Manage 124 (2016) 543–555, https://doi.org/10.1016/j.enconman.2016.07.046. ISSN 0196-8904.
[45] I.P. Holman, Climate change impacts on groundwater recharge- uncertainty, shortcomings, and the way forward? Hydrogeol. J. 14 (2006) 637–647, https://doi.org/10.1007/s10040-005-0467-0.
[46] S. Madhu, G.M. Lionus Leo, P. Prathap, Yuvarajan Devarajan, Ravikumar Jayabal, Effective utilization of waste pork fat as a potential alternate fuel in CRDI research diesel engine – Waste reduction and consumption technique, Process Saf. Environ. Protect. 172 (2023) 815–824, https://doi.org/10.1016/j.psep.2023.02.057.
[47] A.P. Sasmito, E. Birgersson, K.W. Lum, A.S. Mujumdar, Fan selection and stack design for open-cathode polymer electrolyte fuel cell stacks, Renew. Energy 37 (1) (2012) 325–332, https://doi.org/10.1016/j.renene.2011.06.037. ISSN 0960-1481.
[48] S. Padmanabhan, Y. Devarajan, D.B. Munuswamy, S. Sathiyamurthy, C. Selvam, Graphene-enhanced sustainable fuel from Calophyllum inophyllum for premixed charge compression ignition engines: Advancing circular economy and emission reduction, Res. Eng. 24 (2024) 103096.
[49] Y. Devarajan, C. Selvam, Utilization of Sterculia foetida Oil as a Sustainable Feedstock for Biodiesel Production: Optimization, Performance, and Emission Analysis, Res. Eng. (2024) 103196.
[50] Wei Su, Changqing Cai, Ping Liu, Wei Lin, Baorui Liang, Hui Zhang, Zhiliang Ma, Hongzhi Ma, Yi Xing, Weimin Liu, Supercritical water gasification of food waste: effect of parameters on hydrogen production, Int. J. Hydrogen. Energy 45 (29) (2020) 14744–14755, https://doi.org/10.1016/j.ijhydene.2020.03.190. ISSN 0360-3199.
[51] R. Adhinarayanan, A. Ramakrishnan, G. Kaliyaperumal, M. De Poures, R.K. Babu, D. Dillikannan, Comparative analysis on the effect of 1-decanol and di-n-butyl ether as additive with diesel/LDPE blends in compression ignition engine, Energy Sources, Part A: Recovery, Util. Envr. Effects 46 (1) (2024) 9211–9228.
[52] S.M. Veeraraghavan, M.V. De Poures, G. Kaliyaperumal, D. Dillikannan, Waste-recovered quaternary blends: Enhancing engine performance through hydrogen induction by varied injection timing and pressure for sustainable practices, Intl. J. Hydrogen Energy 87 (2024) 227–237.
[53] Nimas M.S. Sunyoto, Mingming Zhu, Zhezi Zhang, Dongke Zhang, Effect of biochar addition on hydrogen and methane production in two-phase anaerobic digestion of aqueous carbohydrates food waste, Bioresour. Technol. 219 (2016) 29–36, https://doi.org/10.1016/j.biortech.2016.07.089. ISSN 0960-8524.
[54] P. Pagliaccia, A. Gallipoli, A. Gianico, D. Montecchio, C.M. Braguglia, Single stage anaerobic bioconversion of food waste in mono and co-digestion with olive husks: impact of thermal pretreatment on hydrogen and methane production, Int. J. Hydrogen. Energy 41 (2) (2016) 905–915, https://doi.org/10.1016/j.ijhydene.2015.10.061. ISSN 0360-3199.
[55] Jishi Zhang, Qinqing Wang, Jianguo Jiang, Lime mud from paper-making process addition to food waste synergistically enhances hydrogen fermentation performance, Int. J. Hydrogen. Energy 38 (6) (2013) 2738–2745, https://doi.org/10.1016/j.ijhydene.2012.12.048. ISSN 0360-3199.
[56] Yunqin Lin, Shubin Wu, Dehan Wang, Hydrogen-methane production from pulp & paper sludge and food waste by mesophilic–thermophilic anaerobic co-digestion, Int. J. Hydrogen. Energy 38 (35) (2013) 15055–15062, https://doi.org/10.1016/j.ijhydene.2012.01.051. ISSN 0360-3199.